Estimating eustasy and ice volume from backstripped low-latitude stratigraphy

M.A. Kominz[1] and S.F. Pekar[2]

[1]Department of Geosciences, Western Michigan University, 1187 Rood Hall, Kalamazoo, Michigan 49008-5150, USA (michelle.kominz@wmich.edu)
[2] Queens College, City University of New York, Flushing, NY 11367, USA and Lamont-Doherty Earth Observatory of Columbia University, Palisades, NY 10964-8000, USA (stephen.pekar@qc.cuny.edu)

Summary The purpose of this guide is to illustrate that with a two-dimensional, sequence-stratigraphic data set and detailed paleobathymetry in a thermally subsiding, tectonic regime, it is possible to extract the eustatic signal at the scale of half-million year variations and therefore place constraints on ice volume changes. While other causal factors in eustatic change are indoubably influencing the eustatic record, they are either relatively minor and within the uncertainties of this method (e.g., thermal expansion and contraction of seawater) or occur at more than the million year time scale (e.g., tectno eustasy).

Citation: Kominz, M.A.and S.F. Pekar (2007), Estimating eustasy and ice volume from backstripped low-latitude stratigraphy, *in* Antarctica: A Keystone in a Changing World – Online Proceedings of the 10th ISAES, edited by A.K. Cooper, C.R. Raymond, et al., USGS Open-File Report 2007-1047, MWR02A, 19 p..

Introduction

One of the most critical and intractable problems in stratigraphy is the extraction of intertwined eustatic (global sea level) and tectonic signals. Despite attempts in the last few decades to separate the effects of tectonics from eustasy, (e.g., Kominz et al., 1998; Sahagian and Jones, 1993; Reynolds et al., 1991; Watts and Steckler; 1979, Bond, 1979; Vail and Mitchum, 1977; Haq et al., 1987; Greenlee and Moore, 1988) significant problems remain (e.g., Christie-Blick and Driscoll, 1995; Christie-Blick, 1991; Steckler et al., 1999).

The extraction of these two signals from the stratigraphic record of transgressive and regressive facies is of considerable importance. An eustatic curve would make an outstanding chronostratigraphic tool (e.g., Haq et al., 1987). Knowing the part of any given stratigraphic record, which is tectonic rather than eustatic would be instrumental in interpreting facies relations and in predicting the presence of source and/or reservoir horizons. The eustatic signal would provide an important reference against which to determine the tectonic signal in a complex tectonic regime. Finally, a significant portion of this eustatic signal is often tied to continental ice sheets and climate (Miller and Fairbanks, 1985; Miller et al., 1987; 1991), therefore, knowing the eustatic history would provide important clues to the Earth's climatic past and cryospheric history (Miller et al., 1991; Zachos et al, 1992).

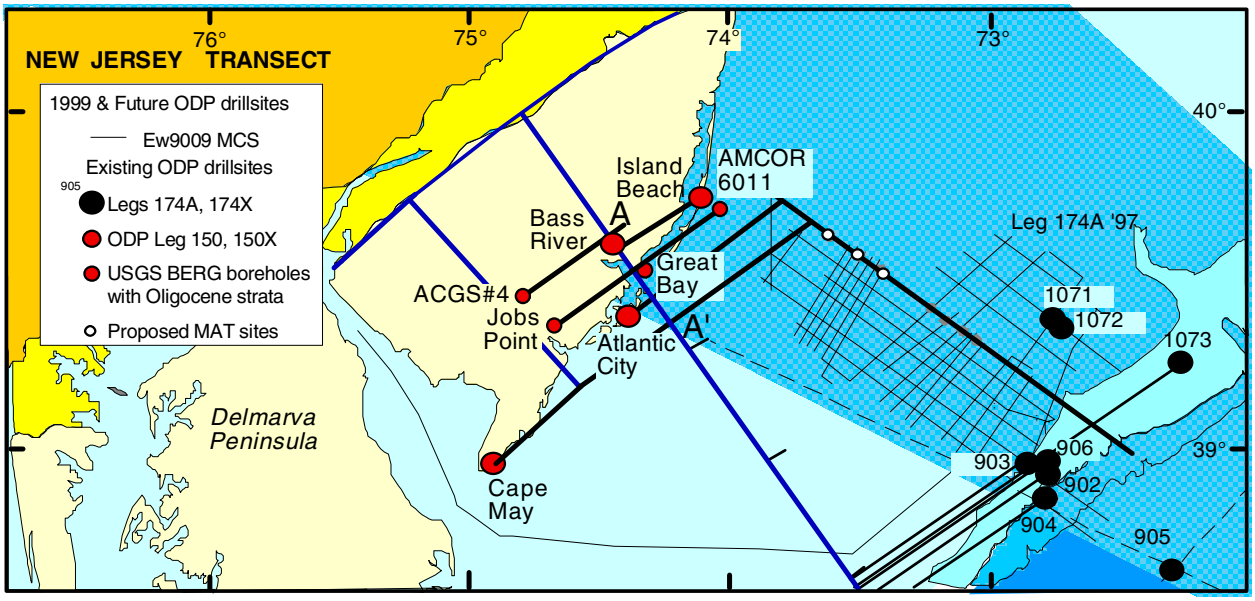

Figure 1. Base map of the southern part of New Jersey. Included are the onshore boreholes from Leg 150X (Island Beach, Atlantic City, and Cape May) and Leg 174AX (Ancora, Bass River, and Ocean View) and offshore sites from Legs 150 (Sites 902-906) and 174A (Sites 1071-1073). Also included are other onshore and offshore wells used in this study: AMCOR 6011, ACGS#4, Great Bay, and Jobs Point. Dip lines are shown and strike lines are projected from the onshore wells onto the seismic line (modified from Pekar, 1999).

The data base

The data needed for this method is stratigraphy deposited in shallow waters on passive continental margins. A series of boreholes are needed that either are located along a dip profile or can be extrapolated along strike to form a dip profile. In the example shown here, the primary data for this work was from boreholes drilled on the New Jersey Coastal Plain (Figure 1), as a part of Ocean Drilling Project (ODP) Legs 150X and 174AX. To constrain the flexural loading effects from far field, offshore wells are also needed. When projected onto a dip profile, they should encompass from landward of the hinge zone to the slope. In the NJ study, ODP sites 902, 903, 906 (Miller and Mountain, et al., 1996) and 1073 (Austin, Christie-Blick, Malone, et al., 1998) were used (Figure 1). The data from the onshore and near-shore wells and boreholes were projected into a single, 32 km composite dip section, which was extended to 170 km to include the offshore well data (Figure 1).

High-resolution age control is needed to correlate the boreholes. In the Oligocene sequence, ages were derived from a combination of Sr-isotope chemostratigraphy, biostratigraphy and magnetostratigraphy (Pekar et al, 2000; Figure 2). These data were combined within a sequence stratigraphic framework to estimate the ages of sequence boundaries and maximum flooding surfaces (Figure 3). While individual absolute age estimates yielded uncertainties on the order of ± 0.3 to ± 0.7 m.y., the combined data set, and sequence stratigraphic framework resulted in age estimates with a relative precision of about ± 0.1 m.y. That is, within any given sequence, the relative stratigraphic correlation was considerably more precise than the absolute age uncertainty (Figure 2). As such, our results could be shifted, somewhat, to older or younger ages, requiring extension or compression in time. The magnitudes and relative positions (in time) of each sequence were not impacted by this uncertainty.

To reconstruct the stratal geometry of the margin, subsidence from compaction, flexural loading, and thermal subsidence need to be quantified. Porosity curves can be used to decompact the sediment (Figure 4). As sediments are progressively buried, the weight of the overburden to compact the sediments owing to waters being squeezed out and

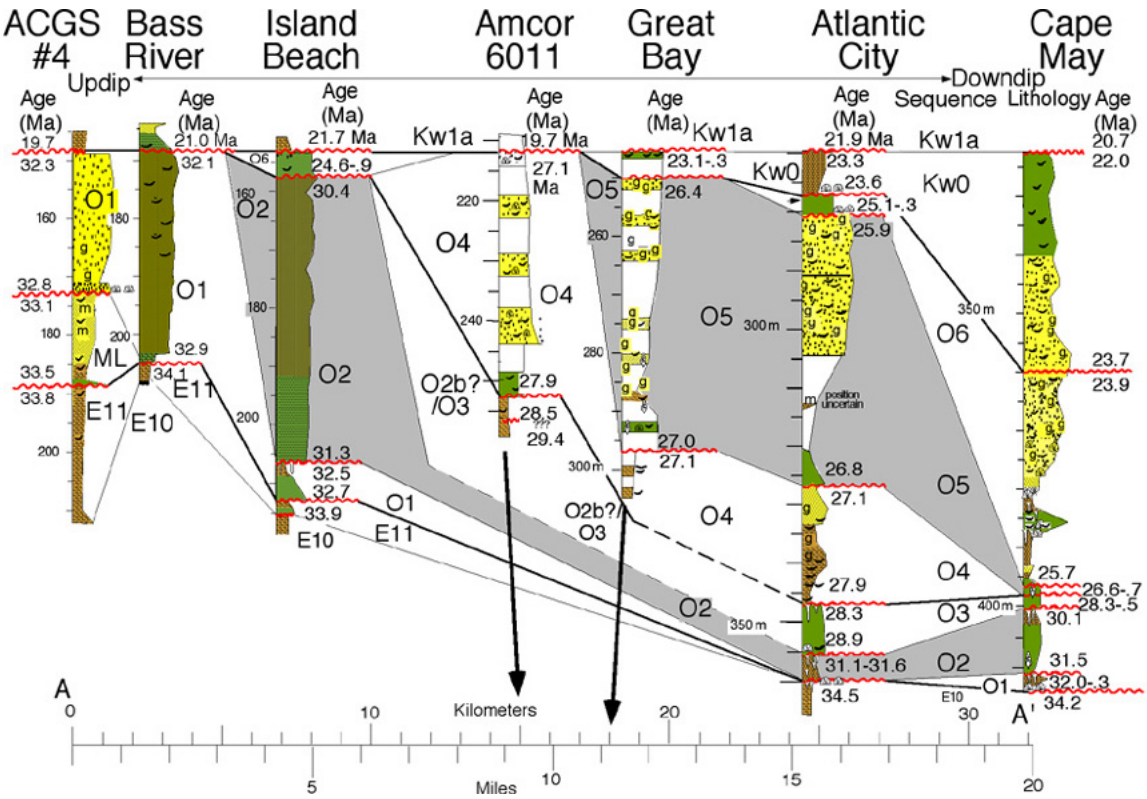

Figure 2. Distribution of New Jersey Oligocene sequences and borehole locations projected onto dip section A-A´ (see Fig. 1), with datum at base of sequence Kw1a. Depths are in meters. Ages of sequences: E10 and E11 are latest Eocene (Browning et al. 1997); ML and O1 to O6 are Oligocene (Pekar et al. 2000); and Kw0 and Kw1a are earliest Miocene (Miller et al. 1997). Successive sequences are arranged laterally, with the oldest landward and the youngest seaward. Also shown are lithology, ages of strata immediately below and above sequence boundaries, and lithostratigraphy (from Pekar et al. 1997). Sequences O2 and O5 are shaded to emphasize correlations between boreholes.

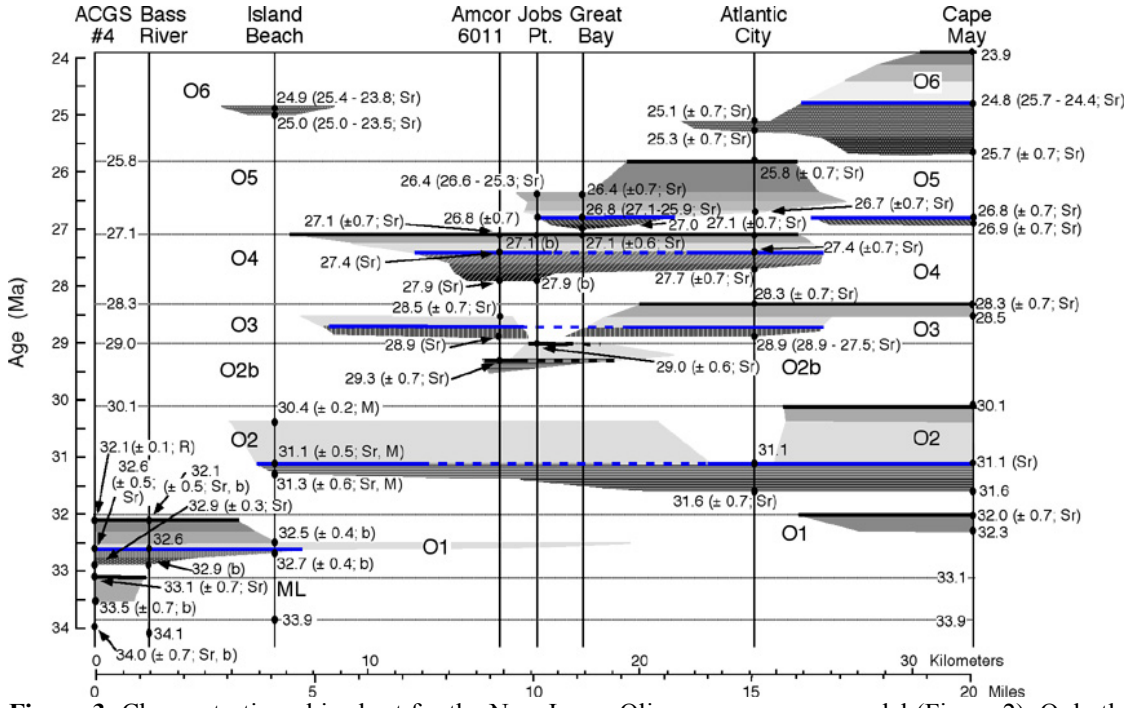

Figure 3. Chronostratigraphic chart for the New Jersey Oligocene sequence model (Figure 2). Only the minimum and maximum age estimates (in millions of years) of each sequence in each well are shown. Error ranges for Strontium isotope ages (Sr) were generally ± 0.7 m.y. Multiple estimates at a single sample location often reduced this error range. The letter "b" beside the date indicates biostratigraphic age estimates. The letter "M" indicates magnetostratigraphic control. Where no uncertainty range is given, that age was extrapolated from data (not shown) within the sequence. Where no indication of the source of age control is given beside the date, it is based on a combination of the above methods. Data shown here is from Pekar et al. (2000) and represents only a small subset of the age control.

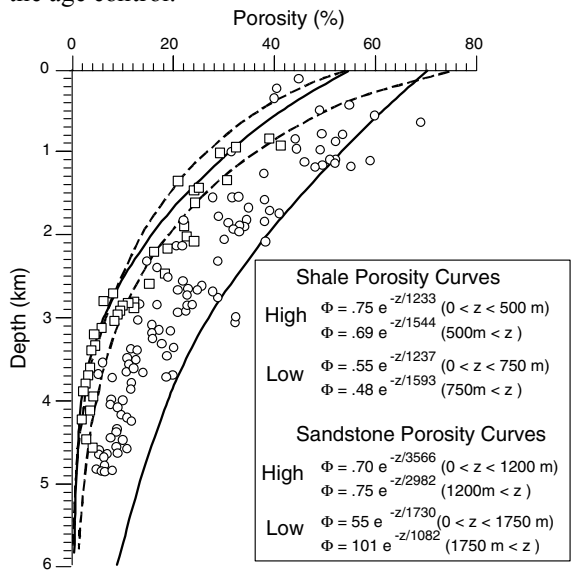

Figure 4. In the New Jersey study, sandstones, shales and glauconite dominated the Oligocene sequences (Figure 2). Glauconite was assumed to compact in the same manner as sandstone. Porosity vs. depth curves for sandstone and shale (Figure 3) were taken from estimates at the COST B-2 well (located on Figure 1; Rhodehamel, 1977; Smith et al., 1976). Porosity estimates for silt, and carbonates (rare in the Oligocene, but more important in Mesozoic strata) were from the generic curves of Bond and Kominz (1984). Sandstone and shale porosity vs. depth curves and equations used in the backstripping analyses compared to data from the Cost B3 well (Rhodehamel, 1977; Smith et al., 1976). Each bracketing set of porosity curves is composed of two exponential equations.

tighter packing arrangements of the sediments. We characterized compaction for each lithology by definition of two exponentially decreasing curves for each lithology following Bond and Kominz (1984). The range of porosity observed for each lithology was taken into account by performing the entire analysis, from backstripping through eustatic sea-level estimates, using first a high end-member and then a low end-member set of porosity curves.

Benthic foraminiferal biofacies and lithofacies are the best means to estimate water depth changes. Typically traditional factor analysis techniques are used to extract the biofacies or lithofacies from the data set. In the New Jeresy, study Q-mode factor analysis was used on samples (capital letters in Figure 5). The calibration of the biofacies

to water depth was accomplished using the two-dimensional backstripping results. The calibration was critical to the sea-level estimates. Because of this, and to alleviate fears that the eustatic estimates are derived by circular reasoning; the calibration is discussed briefly below but is elaborated below and in Pekar and Kominz (2001).

Thick lines connecting the wells are sequence boundaries, while dashed lines are maximum flooding surfaces. Sediments below maximum flooding surfaces, transgressive deposits (Pekar et al., 1999), are depicted with dark to lighter grays, while those above (highstand deposits) are depicted by lightest to darker grays. Surfaces indicated by shading within systems tracts are generated by interpolation between dated intervals on each borehole (Pekar et al., 2000; and Figure 2), and indicate the physical surfaces used in our analyses.

Backstripping procedure

Once an age model has been established with correlation between wells based on a sequence stratigraphic framework (Figures 2-3; Pekar et al., 2000; Pekar 1999), the paleo-topography of the margin can be reconstructed using backstripping procedures. Ideally, the data set would be complete to basement. However, this was not the case for the Oligocene sequences modeled by Kominz and Pekar (2001) (Figure 6). Thus, we need to determine several critical factors including: 1) The margin profile prior to deposition of the Oligocene sequences; 2) The decompacted thickness of the sediment section at the end of the Eocene; 3) The amount of compaction of the underlying sediments as the Oligocene sequences were deposited; 4) The flexural response to the load as the Oligocene sediments were deposited;

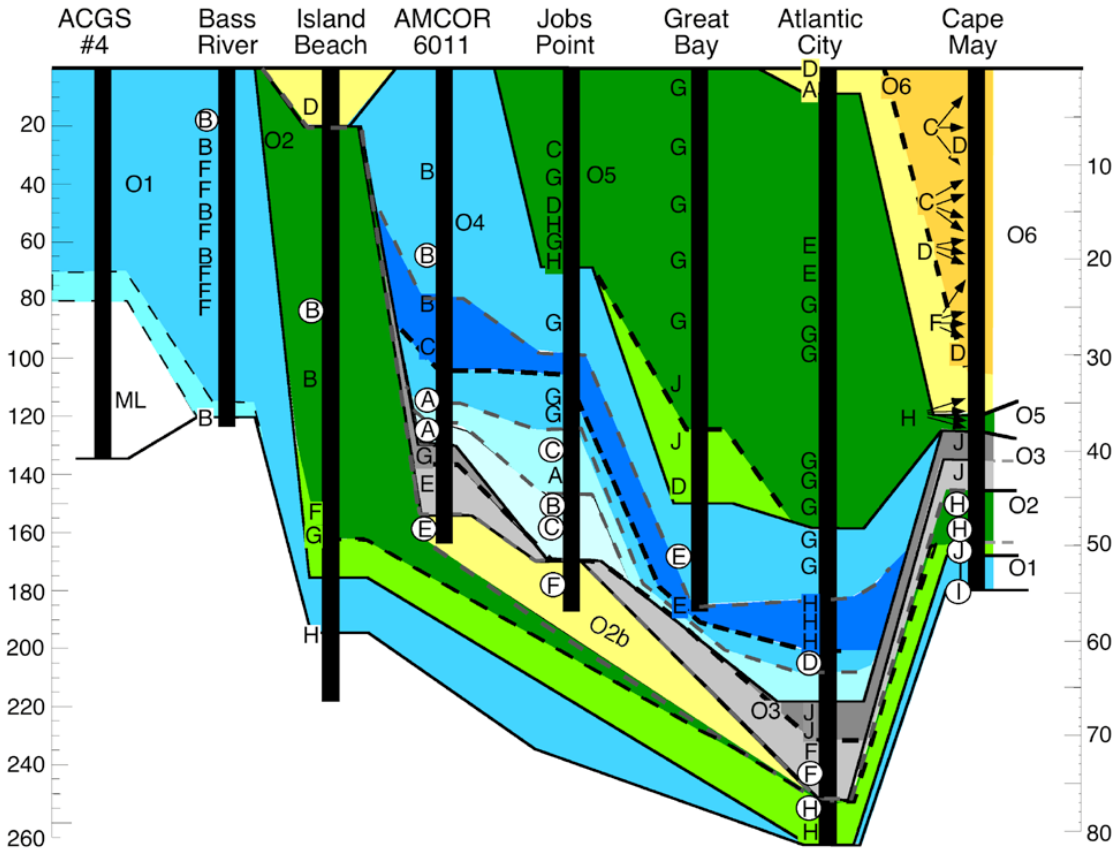

Figure 5. Distribution of sequences used in this study. Sequence names are Mays Landing (ML) and Oligocene1 (O1) through Oligocene6 (O6). Observed thickness and gross lithologies are sketched for each borehole (see Pekar et al., 2003 for detailed lithology). The borehole data are hung from the top of the Oligocene, except the Cape May borehole, which consistently includes more distal, deeper-water units. As such, its base is drawn roughly at the base of the Oligocene section in the adjacent Atlantic City borehole. Because the sediments are not decompacted, it is impossible to generate a realistic cross section. Borehole data are plotted according to their projected horizontal locations on the dip line shown in Figure 1. Capitalized letters to the left of each well give the locations of benthic foraminiferal biofacies, obtained by factor analysis and calibrated by application of two-dimensional backstripping (Pekar and Kominz, 2000). The deepest biofacies observed is designated by J; the shallowest is A.

and 5) The tectonic subsidence of the margin. The procedure is dependent, in large part, on sediment thickness and density, obtained from one- dimensional backstripping. In contrast, it is fully independent of a priori Oligocene paleo-bathymeteric estimates.

Establishing the paleoslope gradient

An estimate of the paleoslope gradient is required. Although estimates of paleogradient of passive margins can be controversial, estimates of the factors (e.g., sediment input, subsidence rates) that control the slope of the margin can be used as constraints. For example, in New Jersey, while previous estimates assumed paleoslope gradients similar to the present (1:1000) (Browning et al. 1997), two-dimensional backstripping indicates that paleoslope gradients ranged from 1:500 (landward of the hinge line) to 1:300 (seaward of the hinge line) for the shelf during the Paleogene (Steckler et al. 1999; Pekar 1999) (Figure 7). This higher paleoslope gradient was due to low sediment input creating a sediment-starved margin, resulting in increasing water depths along the margin during the Paleocene through the early Oligocene.

Estimating sediment compaction

Determining the decompacted thickness of the sediment section at the end of the Eocene, the amount of compaction of the underlying sediments as the Oligocene sequences were deposited and the thickness of the Oligocene sediments themselves are achieved through one-dimensional geohistory analysis (Van Hinte 1970?). Geohistory analysis restores sediment thickness through time using lithology-dependent porosity vs. depth curves (Figure 4) (e.g., Rhodehamel, 1977; Smith et al., 1976; Bond and Kominz, 1984). In our model, compaction for each lithology is characterized by definition of two exponentially decreasing curves for each lithology following Bond and Kominz (1984; e.g., Figure 4).

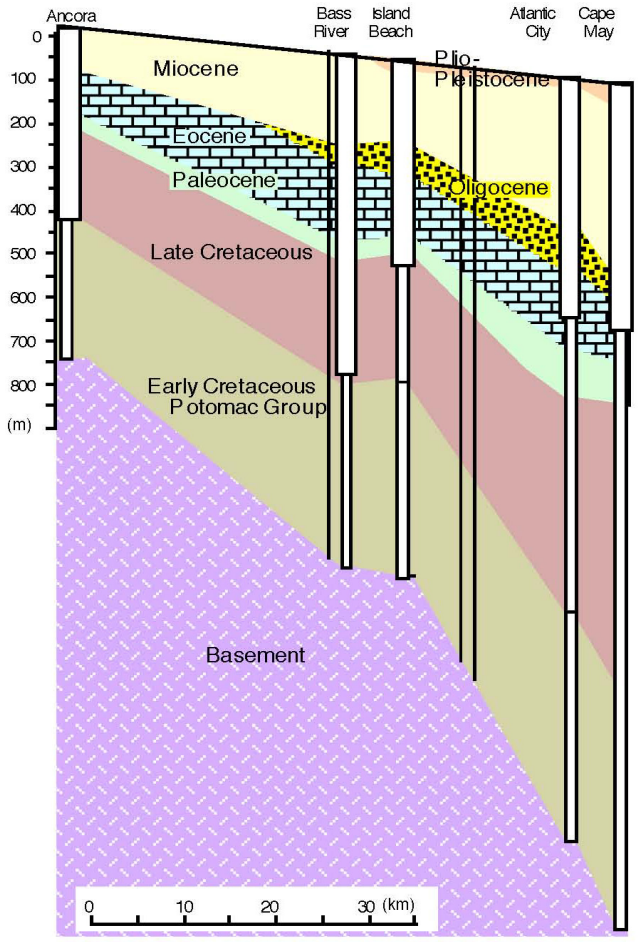

Figure 6. In the New Jersey, study the sequence stratigraphic model includes only the Oligocene strata which is underlain and overlain by additional coastal plain sediments. Thus, the compaction effects of these sediments must be taken into account in order to obtain the geometry of the Oligocene sediment packages through time. In the figure wide white rectangles represent ODP boreholes (80-90% core recovery) while narrow rectangles and vertical black lines represent boreholes for which cuttings were available. Figure from Kominz and Pekar 2002.

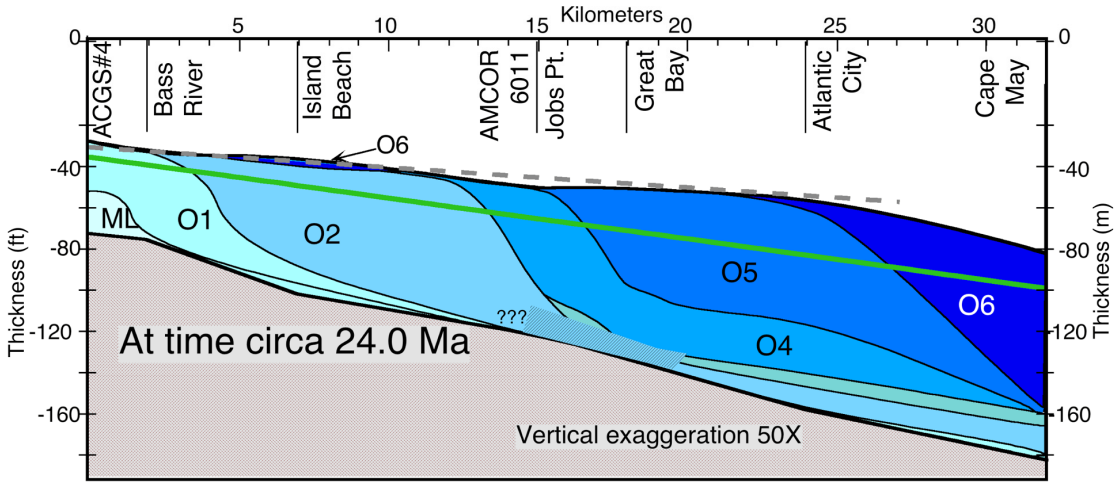

Figure 7. Distribution of New Jersey Oligocene sequences projected onto dip section A-A' (see Fig. 1) at ~ 24 Ma. Sequences ML and O1 through O6 are of Oligocene age. Ties for reconstructed sequence boundaries are depths at each borehole. Clinoforms are required by the data; the sigmoidal shapes are conjectural. Clinoform relief is inferred from two-dimensional flexural backstripping (Kominz and Pekar 2001). Bold green line indicates original depth and gradient (1/500) of Eocene-Oligocene surface. Bold gray dashed line indicates paleoshelf gradient landward of rollover (1/1000).

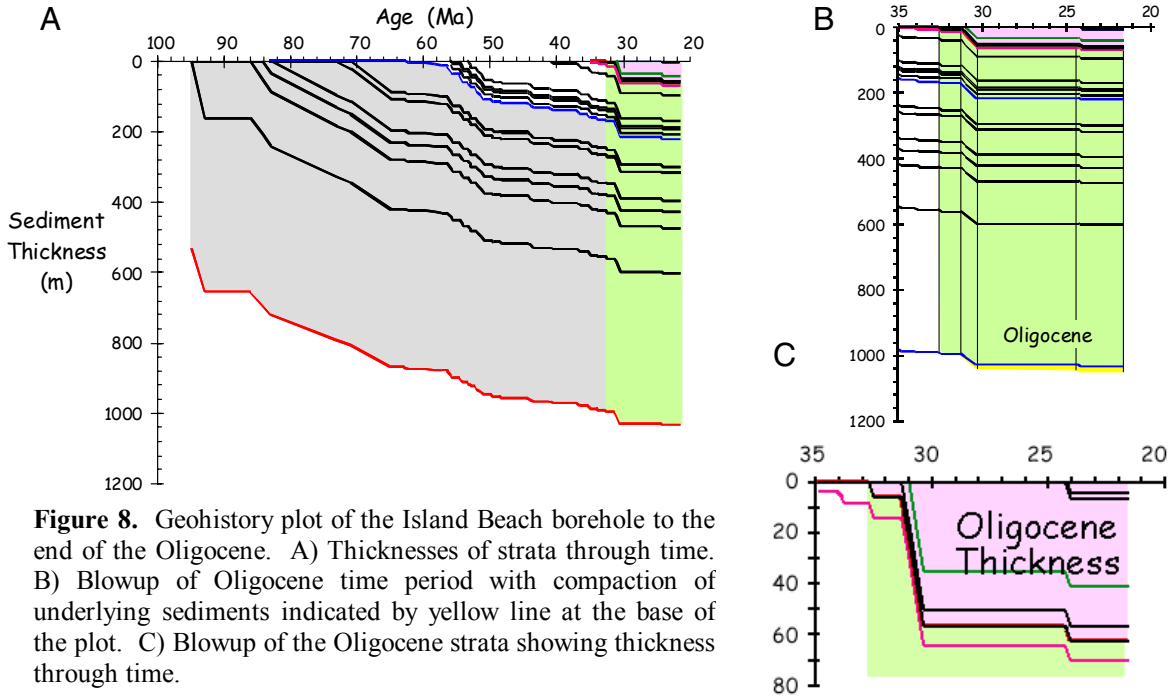

Figure 8. Geohistory plot of the Island Beach borehole to the end of the Oligocene. A) Thicknesses of strata through time. B) Blowup of Oligocene time period with compaction of underlying sediments indicated by yellow line at the base of the plot. C) Blowup of the Oligocene strata showing thickness through time.

The range of porosity observed for each lithology is determined by using first a high end-member and then a low end-member set of porosity curves. The geohistory plot from the Island Beach borehole is provided as an example in Figure 8. These data are used to determine the change in total sediment thickness as the Oligocene sediments loaded the older strata and the thickness and density of the Oligocene section for flexural calculations.

Constraining the flexural response to sediment loading and thermal subsidence

A two-dimensional flexural model is needed to calculate the response of the basement to the sediment load of the section being studied. The sediment section (from both the onshore and offshore wells) is progressively loaded onto an elastic plate. The response of the plate is to bend. The accommodation space generated by the bending plate is added to that obtained from compaction of underlying sediment, the new sediment is added and the geometry of the margin is obtained.

For New Jersey, we assumed that the rigidity landward of the hinge zone was equal to that of a 33 km thick elastic plate.

$$D = \frac{ETe^3}{12\left(1-\nu^2\right)} \qquad \text{Equation 5}$$

where: D = Flexural rigidity

E= Young's modulus = 6.5×10^{10} N/m^2

n = Poisson's ratio ≈ 0.25

Te = elastic thickness

For the plate beneath the New Jersey study sites Te = 30 km

$$D = \frac{6.5x10^{10}\,N/m^2\left(3.0x10^4\,m\right)^3}{12(0.9375)} = 1.56x10^{23}\,Nm$$

In our study, we decreased the rigidity to a 20 km elastic plate thickness near the shelf-slope break (Figure 9) located at 150 km on the composite dip section, (Figure 1). In this case considerable cooling of the lithosphere had occurred prior to the Oligocene, due to about 125 m.y. of cooling. By this time cooling was slow, so we did not vary rigidity with time.

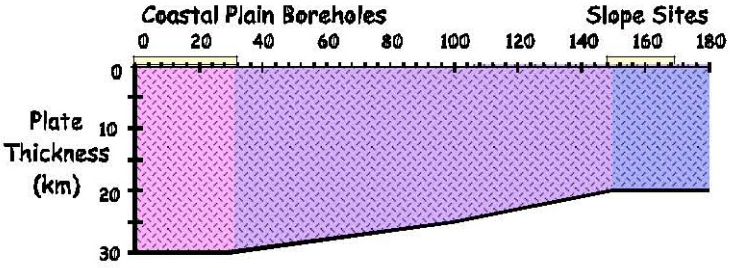

Figure 9. Rigidity model for cross section studied off the coast of New Jersey. Beneath the coastal plain boreholes is unstretched continental crust, while crust beneath the slope sites was stretched extensively.

To calculate the basement response of an elastic plate with rigidity D at a distance x from a line load, L is:

$$w = \frac{L\alpha^3}{8D} e^{-x/\alpha}\left(\cos\frac{x}{\alpha} + \sin\frac{x}{\alpha}\right) \qquad x > 0 \qquad \text{Equation 6}$$

where a is the flexural parameter:

$$\alpha = \left(\frac{4D}{\rho_a - \rho_w}\right)^{1/4} \qquad \text{Equation 7}$$

and r = density, a = asthenosphere, and w = water.

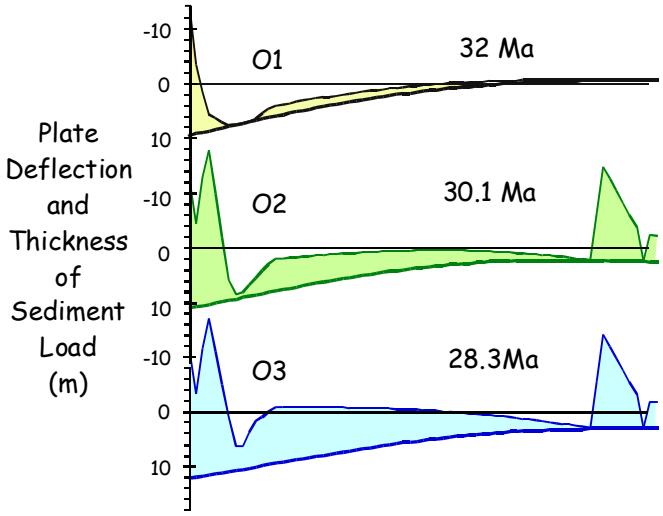

Figure 10. Several examples of the deflection of the plate beneath the sediment load are shown. Sediment packages are fully lithified and include all sediment beneath the top of sequence O1, O2 and O3, respectively. Note that the geometry of the margin is not correct. In particular, thick sediments seaward of the shelf-slope break appear as thick wedges. From Kominz and Pekar, 2002.

The Oligocene stratigraphy was actually divided into 0.1 m.y. increments and sequentially placed on the rigidity model above. A few examples of the deflection at the end of sequence O1, O2 and O3 are shown in Figure 10. Sediment thicknesses were interpolated between wells. Only the coastal plain portion of the results was used in our model.

Constraining the tectonic subsidence

In a passive margin setting, tectonic subsidence of the basement generally increases with distance away from the continent. In general, the tectonic subsidence would generate accommodation space that must be taken into account in recreating the margin geometry. In the general case, the tectonic subsidence would be estimated by backstripping to generate R1, the first reduction:

$$R1 = S\,\frac{\rho_a - \rho_{s*}}{\rho_a - \rho_w} + Wd = TS + \Delta SL\,\frac{\rho_a}{\rho_a - \rho_w} \qquad \text{Equation 8}$$

where: ΔSL = eustasy,
R1 = accommodation,
S* = decompacted sediment thickness,
WD = paleodepth,
and ρ = density, a = asthenosphere, and w = water.

R1 is then fit to theoretical thermal subsidence models (e.g., McKenzie 1978) to determine the thermal subsidence. The accommodation space due to thermal subsidence is then added to the accommodation space generated by compaction and by loading of the elastic plate.

The subsidence beneath the coastal plain, which is landward of the hinge zone, is generated by flexural response to sediment loading of the cooling, stretched, seaward portion of the margin (e.g., Steckler et al., 1988). As such, this component of subsidence was taken into account by the two-dimensional loading model, which included offshore sediment loading (Fig. 10). Thus, tectonic subsidence was not included as a separate source of subsidence in this study. Two-dimensional backstripping was used to estimate the geometry of each surface from up-dip to down-dip and its vertical relation relative to older and younger horizons.

Oligocene sequence geometry

After the pre-Oligocene gradient is corrected for sediment compaction, basement response to the load and tectonic subsidence the Oligocene sediments are placed on the subsiding surface to obtain the geometry of the sequences. This gives the relationship of each sequence surface to other surfaces through time (Figure 11) (Kominz and Pekar, 2001;

Kominz and Pekar, 2002). Once these relations are known, the paleo environmental indicators are also indicators of sea-level change.

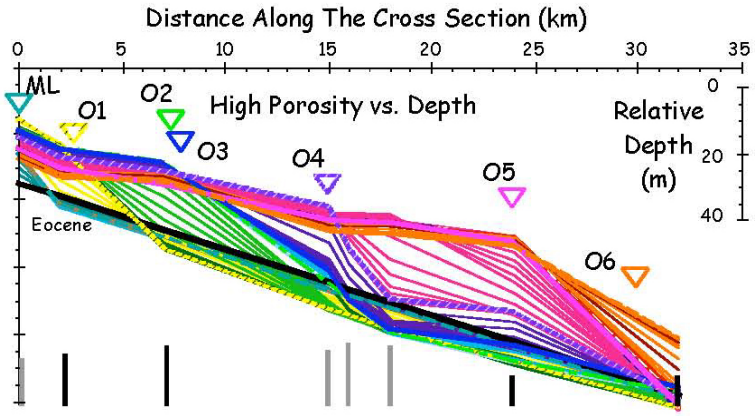

Figure 11. Flexural backstripping predicts the geometry of the margin as it evolved through time. Each thin line represents a 0.1 m.y. interpolated, profile. The sequence boundaries are thick lines with their offlap break indicated by an inverted, triangle, and labeled as that sequence. (Kominz and Pekar, 2002).

Introduction to using benthic foraminiferal biofacies as paleo water depth indicators

Although the distribution of benthic foraminifera is constrained by the environmental conditions in which they live and not by water depth, these environmental conditions (e.g., substrate, salinity, temperature, wave energy, oxygenation, nutrients, etc.) are often depth-dependent (e.g., Walton 1964). This has enabled workers to use foraminiferal assemblages as paleobathymetric indicators. However, studies comparing benthic biofacies assemblages on shelves in different basins (e.g., Bandy 1964; Walton 1964; Sen Gupta and Kilborne 1976) indicate that although the relative positions of benthic biofacies assemblages from near shore to the shelf break remain fairly constant, the actual water depths for specific foraminiferal assemblages can vary greatly. This is because particular locales possess unique environmental conditions, including physiographic parameters such as shelf-margin geometry and water depths at the shelf edge. Therefore, water depths for benthic foraminiferal biofacies are distinctive to a particular margin. As a result, benthic foraminiferal paleobathymetric estimates that use data from other margins may contain large uncertainties (Walton 1964).

Paleobathymetries for benthic foraminiferal assemblages have been determined using fossil and modern benthic foraminiferal habitat studies (Bandy 1961; Walton 1964; Murray 1973). This uses trends in foraminiferal abundance, diversity, and other parameters that change with distance from the shoreline and with increasing water depth (Bandy and Arnal 1957, 1960) can provide relative paleodepths. This has been most successful for strata of Neogene age and younger. However, many recent benthic foraminiferal species evolved since the late Eocene (Hayward et al. 1999). Thus, care is needed when comparing Paleogene or older records to modern-day analogs.

Abundances of planktonic foraminifers increase with distance from the shore, suggesting that comparison of planktonic and benthic foraminifers (P/B ratios) can also be a useful estimator of water depth (Stehli and Creath 1964). However, precision in calibrating water depth to P/B ratios has been difficult because of variations in sedimentation rates, planktonic productivity, and dissolution (Lipps et al. 1979).

One-dimensional paleoslope modeling using benthic foraminifers has provided paleodepth estimates for biofacies on margins for various time periods (e.g., Cretaceous, Nyong and Olsson 1984; Miocene, Miller et al. 1997). This method is most useful for margins that contain a geometry similar to the present-day shelf. Therefore, it is limited in terms of scope because paleoslope gradients can vary from 1:300 to 1:500 (as in the case of a carbonate ramp; e.g., Steckler et al. 1999) to < 1:1000 on a typical siliciclastic shelf margin (e.g., present-day New Jersey margin; Bowman 1977). This method also does not take into account nonlinear geometry (e.g., clinoforms) due to variable sediment input and subsidence. Although the methods mentioned above have generated useful estimates of paleobathymetry on a given margin, the large uncertainties suggest that an improved method of estimating water depths of benthic foraminifers is needed.

Two-dimensional paleoslope modeling of the foraminiferal biofacies

A major difficulty in generating a paleoslope model for the New Jersey Oligocene strata is the presence of clinoforms. The nonlinear slope makes it impossible to estimate paleodepths using a one-dimensional model.

However, by using two-dimensional backstripping paleo reconstruction of the stratal geometry of passive margins can be accomplished (e.g., Fig. 11).

As discussed above, although the distribution of benthic foraminifera was constrained by the environmental conditions (e.g., substrate, salinity, temperature, wave energy, oxygenation, nutrient) in which they lived and not by water depth, environmental conditions are commonly depth-dependent (e.g., Bandy, 1953; Walton, 1964). Thus, it is possible to construct a model relating water-depth to benthic biofacies (e.g., Nyong and Olsson, 1984; Olsson, 1991; Miller et al., 1997). Additionally, because environmental factors become less variable with increasing depth, such a model must become less precise with depth. A new approach to calibration of benthic biofacies to water depth was made possible by the two-dimensional backstripping results obtained above.

Benthic foraminiferal biofacies that inhabit the shallowest water depths can be used to calibrate foraminiferal biofacies interpreted to have inhabited deeper water depths. In the New Jersey study, three benthic foraminiferal biofacies (A, B and C) were interpreted as indicating inner neritic environments, based on lithostratigraphic relations, previous work on younger, equivalent fauna, and low biodiversity (Pekar and Kominz, 2001) that suggest these biofacies lived in inner neritic environments and, thus, in water-depths of less than 30 m. Relative depths can be obtained where two different biofacies could be correlated along a single time horizon (Figures 12 and 13).

Chronostratigraphic correlation was possible due to the tight age control and the sequence stratigraphic framework. Biofacies A was observed in the Amcor 6011 borehole during early deposition of sequence O4 (Figure 12). Over the same interval, biofacies B, A and C were observed in the Jobs Point borehole. By correlating along the backstripped.

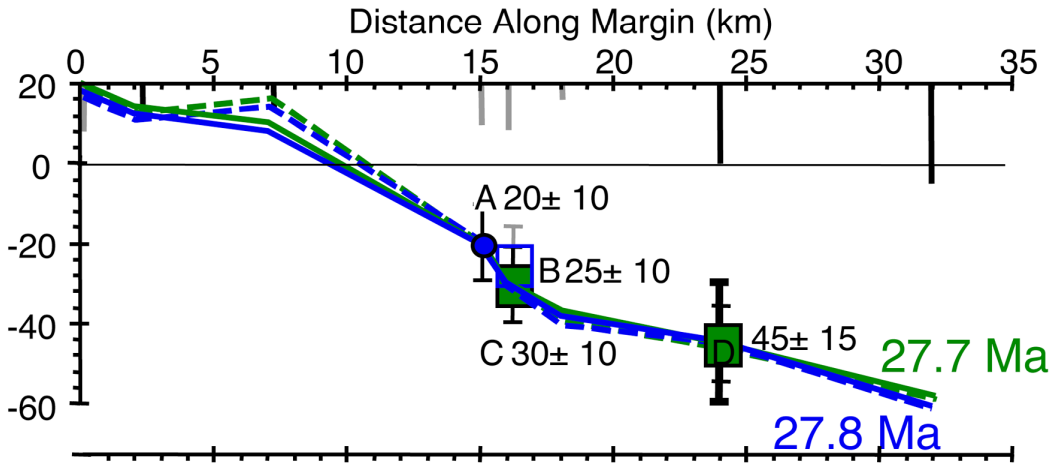

Figure 12. Water-depth ranges of Benthic foraminiferal biofacies constrained by the sediment surface geometries (Pekar and Kominz, 2001). Solid lines are from high porosity curves and dashed lines are from low porosity curves (Figure 4, Pekar and Kominz, 2001). Benthic biofacies assemblage A (circle) was used to constrain the depth of each profile. Error bar indicates range of water depth for that benthic biofacies. Biofacies depths estimated by correlation along these horizons are given by rectangles and labeled by biofacies (B, C and D). Thick error bars are suggested due to reduced environmental variation with depth and are used in sea level modeling.

geometry at 27.8 Ma and 27.7 Ma we found that the surface at the location of Jobs Point was about 10 m deeper than it was at the location of Amcor 6011 during these two intervals of time (Figure 8). Thus, biofacies B and C were assumed to indicate deeper water depths than biofacies A. As the shallowest inner neritic benthic biofacies, A was assigned a water-depth of 20 ± 10 m. The deeper inner neritic biofacies were assigned water-depths of 25 ± 10 m (B) and 30 ± 10 m (C). Paleodepth uncertainties for foraminiferal biofacies were assigned ranges of ± 10 m for the inner neritic (< 30 m); ± 15-25 m for the middle neritic (45-85 m); and ± 30 m for the innermost outer neritic (100-115 m). Because environmental factors become more stable with depth in neritic environments, any model must become less precise with depth

Estimating sea-level change from two-dimensional backstripping results combined with depth-calibrated benthic biofacies

Two-dimensional backstripping provides the geometric relations in time and space along your sequence stratigraphic cross section. Benthic biofacies living at any point along a profile establishes the depths of that entire profile. In the case where the depth control on one profile is inconsistent with that of the next youngest profile, that is, the physical depth relationships are violated by adjacent benthic biofacies a sea-level change is required. On the other

hand, if two benthic biofacies living at the same time require different depths for the same profile and those depths are outside of the error limits of the benthic biofacies, then the profile is incorrect. This means that the backstripping assumptions were incorrect, and, most likely, implies a tectonic event that has not been taken into account in the backstripping model.

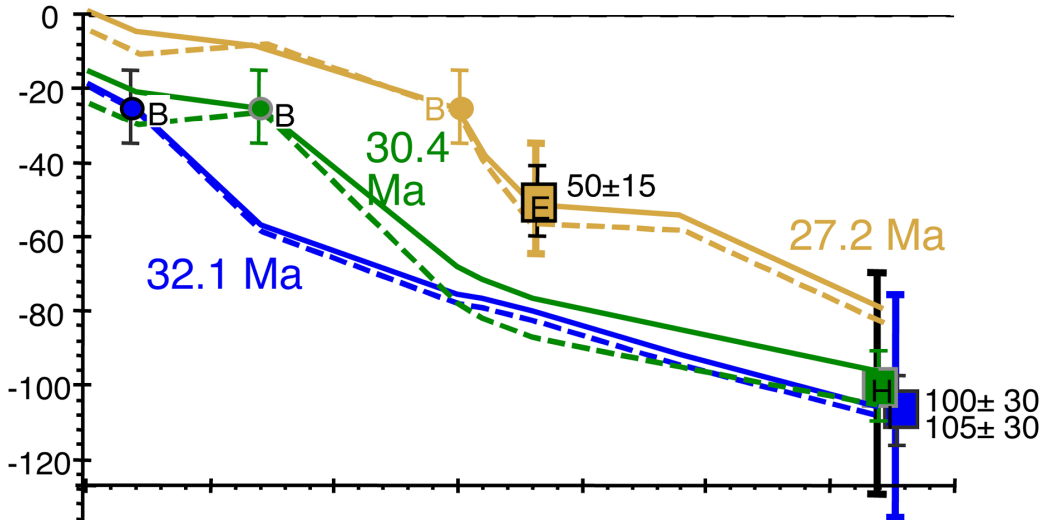

Figure 13. Benthic biofacies assemblage B (circles) was used to constrain the depth of benthic biofacies assemblages E, H and I. Symbols and line patterns as described in Figure 12. For all benthic biofacies the range of water depth uncertainty was designed to generate substantial overlap in the ranges of adjacent benthic biofacies. The ranges were increased with increasing water depth because variations in environment decrease with depth. Deeper-water biofacies (D-J) were assigned water-depth ranges by correlation to inner neritic biofacies based on the sequence stratigraphic model (Figure 5 and 11). The water depth of the inner neritic benthic biofacies (20, 25, or 30 m ± 10 m, see above) was used to constrain the depth of the Oligocene surface at the location of the borehole in which it was observed. That is, the geometry of the profile at that time, generated from backstripping, was hung from the depth required by the inner neritic biofacies (Figure 12). The water-depth in which the deeper-water biofacies lived could then be estimated. This was possible for biofacies D, E, H and I. We already used benthic biofacies A preserved at the Amcor 6011 borehole to establish the relative depth of the sediment surface profile at that time, requiring a water depth at the Atlantic City borehole of 45 ± 10 m (Figure 12). Biofacies H and I are outer-middle to outer neritic and thus were assigned larger depth ranges of ± 30 m. We found that the impact of using high vs. low porosity assumptions was generally small (Kominz and Pekar, 2001).

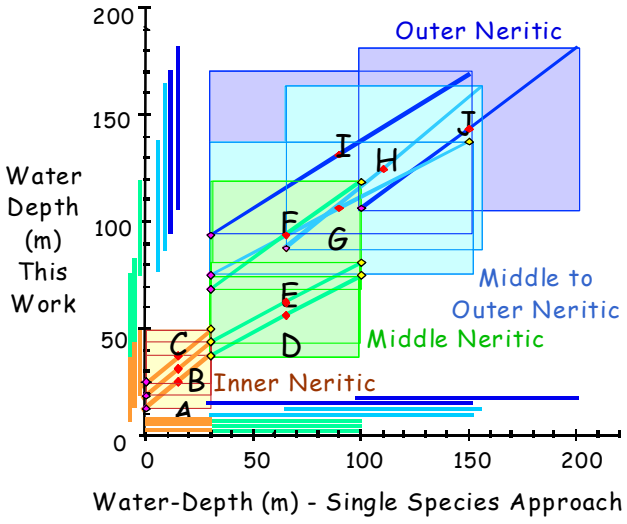

Figure 14. Environments of benthic biofacies assemblages derived from the two-dimensional backstripping approach compared with the environments indicated by the dominant species present in these biofacies. While our model reduces apparent uncertainty, the overall depth distributions of the various benthic species are consistent with the more conservative, single species approach. (from Kominz and Pekar, 2002).

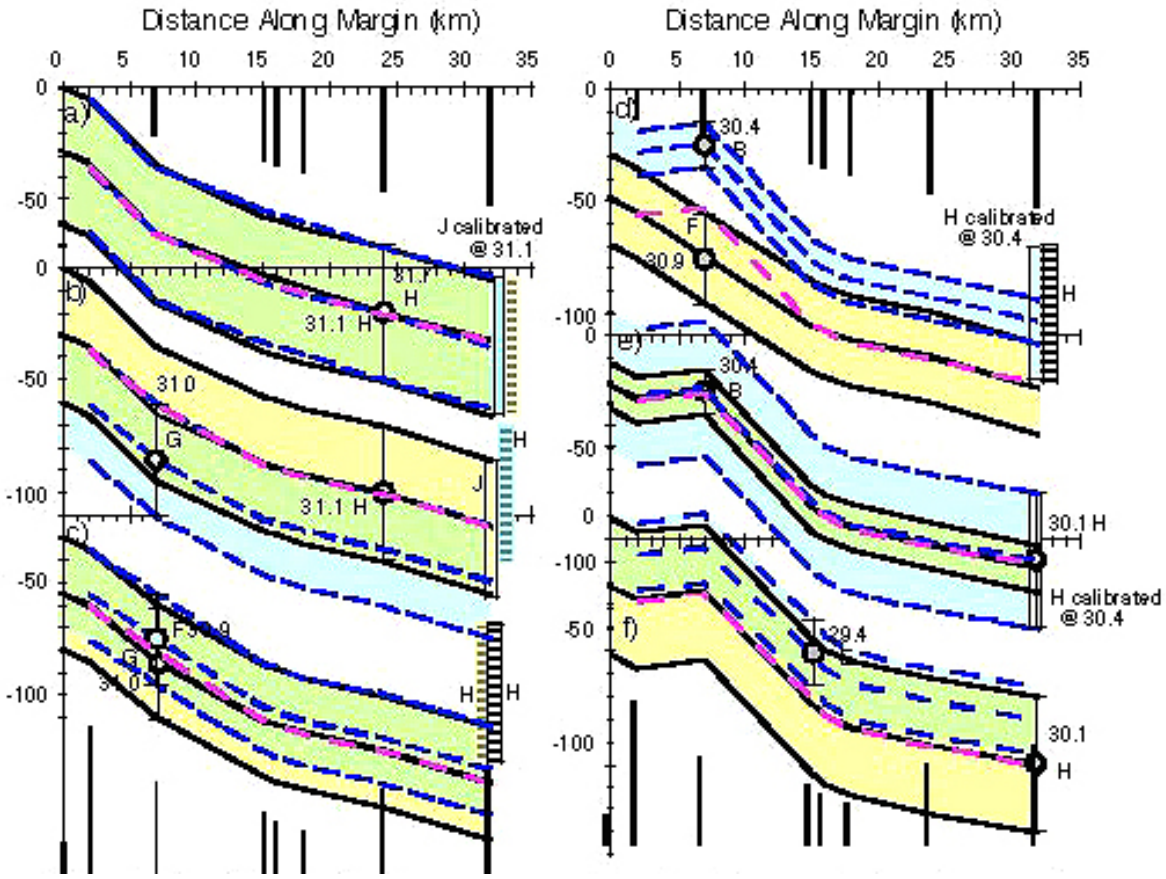

Figure 15. Detailed example of the generation of R2 and eustatic estimates from 2-D backstripping, sequence O2. 10a through 10f each show the geometry of two consecutive time horizons. Circles with error bars show the water depth ranges of the benthic biofacies (indicated by a letter, e.g., G and H in 10b) used to hang the cross section. The older horizon's range of water depths is indicated by solid black lines. The depth range is shaded yellow. The younger horizon's depth range is indicated by dashed blue lines and it's range is shaded light blue. Overlap of the two ranges is green. Pink dashed lines give the depth of the younger horizon relative to the older horizon, as determined by backstripping alone. The difference between the pink dashed line and the blue dashed line is R2, the apparent change in relative sea level, R2. (Kominz and Pekar, 2002).

In the New Jersey case, the two-dimensional backstripping provides the geometric relations in time increments of 0.1 m.y. (Fig. 11). We illustrate the application of benthic biofacies to the backstripped profiles for sequence O2, from 31.1 to 30.1 Ma in Figure 15. In the example of sequence O2, the case in which no sea level change is required is well illustrated by the shift from 31.7 to 31.1 Ma in Figure 15a. In this case both profiles are constrained by benthic biofacies H located at the Atlantic City borehole (25 km along the profile). There is little change in depth required by the backstripping results between 31.7 and 31.1 Ma, thus no sea level change is required between these two time periods. It is interesting to note that benthic biofacies J is present at Cape May (32 km on the profile) at both time periods. Benthic biofacies J was calibrated at 31.1 Ma so it does not constrain the profile depth in any way. However, its' presence at 31.7 Ma is confirmation of the cross section at that time. That is the geometry of the margin as generated by backstripping is consistent with the water depths required by the two benthic biofacies observed in the strata of the Cape May and Atlantic City boreholes at that time.

An example for which a sea-level change is required is illustrated by the change in depths of the profiles from 30.9 to 30.4 Ma (Figure 15d). In this case the profile at 30.9 Ma is constrained by benthic biofacies F located in the Island Beach borehole and the profile at 30.4 Ma is constrained by benthic biofacies B located in the same borehole. The pink dashed line shows that a significant pile of sediments was added in this location, due to the change in shape of the profile between these two time periods. Additionally, the difference in height between the pink and the bold blue

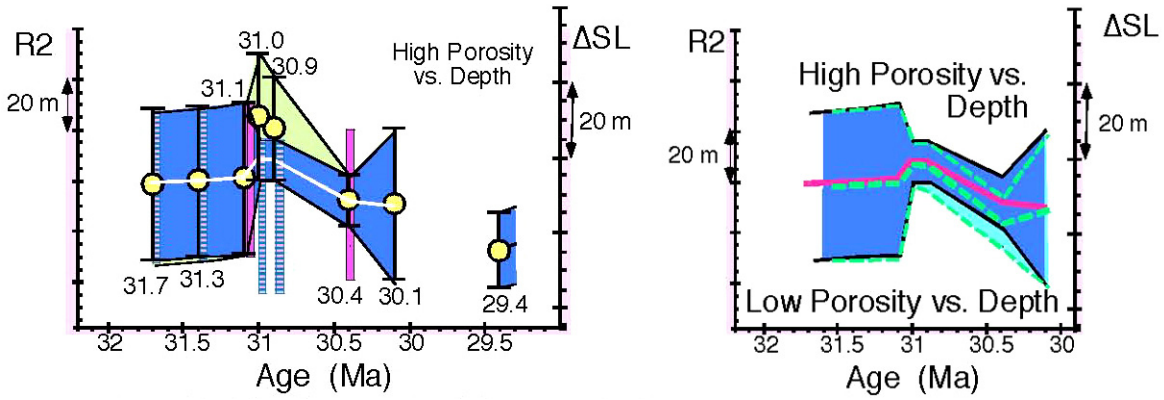

Figure 16. The relative sea level change required by two-dimensional backstripping and benthic biofacies distribution for sequence O2. Note (left) that the sea level range at 30.9 and 31.0 is restricted to the lower portion of the range due to the requirement that benthic biofacies in Cape May and in Island Beach boreholes be consistent. The graph at the right includes results with low porosity vs. depth curves. The entire range including both high and low porosity vs. depth curves is our range of possible sea level change. (Kominz and Pekar, 2002)

dashed line is the required sea-level change. In order to move the older pink profile up to the younger blue profile a sea level fall of about 30 m is required. Benthic biofacies H was calibrated to benthic biofacies B at 30.4 Ma (Fig. 15d and Fig. 13). As such it does not constrain the depth of the profile at that time. However, it's presence at 30.9 Ma restricts the profile depth to only those depths consistent with benthic biofacies F at Island Beach and benthic Biofacies H at Cape May (Figure 16).

It is also important to note that where no benthic biofacies constrain the profiles no sea level change can be estimated. Thus, although the backstripping was performed in 0.1 m.y. increments, the sea-level curve can only be generated where benthic biofacies have been determined in at least one core. The presence of multiple benthic biofacies constraining the sea level change is indicated by the presence of both a yellow dot with black error ranges and a vertical pink and blue bar indicating the presence of a second biofacies at the same time (Fig. 16). The presence of a pink vertical bar indicates that that benthic biofacies was calibrated by that relation and it thus, provides no constraint on sea level at that time. The R2 changes (left scale) are summarized in Figure 16. ΔSL, or eustasy (right scale), is calculated from R2 by removing the effects of water loading. Present-day sea level was not tied to eustasy. The white line represents our best estimate for sea level change and the blue region shows the possible range of sea level change. These results were obtained using the high porosity curves. Dashed lines in Figure 16 show the constrained R2 and eustatic results assuming low porosity vs. depth curves.

Why bother with two-dimensional backstripping?

1) It allows us to take advantage of the two-dimensional variations in stratigraphy that are constrained by the sequence stratigraphic approach.
2) It improves the backstripping itself, but allowing for variations in rigidity of the underlying basement and distribution of the response to the sediment load.
3) It allows us to constrain the water depth range of benthic biofacies by correlation from shallow to deep-water benthic biofacies present contemporaneously.
4) The presence of a single benthic biofacies at any well establishes the depth of that profile at all wells.
5) The presence of multiple, contemporaneous benthic biofacies tests our backstripping model in that inconsistent results would imply active tectonics between the two locations.

Estimating ice volume from the eustatic estimates

Since eustatic estimates include not only ice volume but other eustatic inputs (tectno-eustasy, thermal expansion and contraction, etc.). Of the factors that control eustasy, only glacio-eustasy is both rapid ($<10^6$ yrs) and large (tens of meters of sea-level change). Thermal contraction is typically on the order of a few meters, while tecto-eustasy, while can result in large sea-level changes, is usually on the order of $>10^6$ years (Figure 17). Nevertheless, for longer records, estimates of the affects of long-term eustatic changes from tectonic mechanisms should be estimated. For example, from New Jersey study, during the latest Eocene to earliest Miocene, a 95-meter sea level fall was observed. During this time interval tectno-eustatic effects from decreasing ocean ridge volume (Kominz, 1984), the initiation of the collision of India with Asia began at about 50 Ma (e.g., Harrison, 1990), cooling of the Cretaceous Pacific

volcanism (Schlanger et al., 1981) are estimated to have resulted in a eustatic fall between 20-30 meters (Kominz and Pekar, 2001). At the same time, there is some suggestion of a significant cooling of ocean water, which may have generated a sea-level fall of 2 to 5 meters (Sahagian, 1988). The new eustatic record from Miller et al. (2005), provides some ideas on the extent of tectno-eustasy during the past 100 Ma.

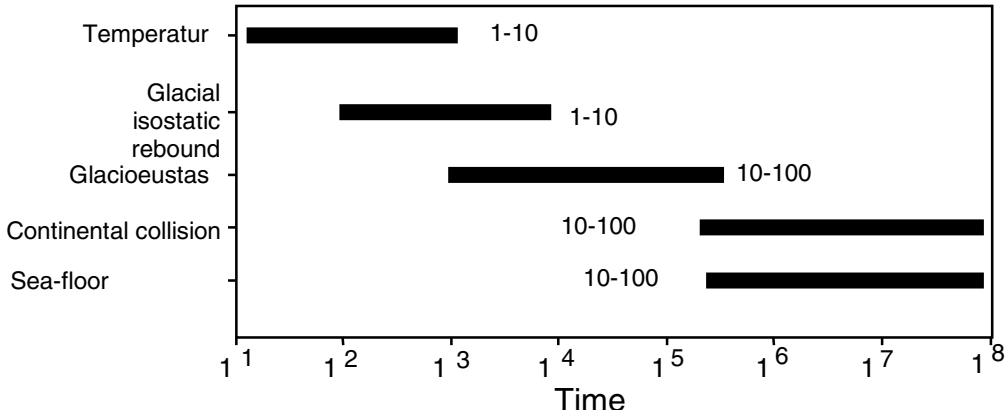

Figure 17. Mechanisms of global sea-level change.

Calibrating isotopic records to glacioeustasy

Fairbanks and Matthews (1978) was the first to calibrate $\delta^{18}O$ to global sea-level changes. They used reef-crest coral *Acropora palmata* as an indicator of near surface waters (<5 m) from uplifted late Pelistocene reefs located in Barbados that lived since the last glacial maximum (~20,000 year ago). They estimated sea-level rise by calculating the height of uplifted coral terraces and by assuming a constant uplift of the area. Dating was done using $230^{Th}/234$ U age estimates. Oxygen isotopes were obtained from the same corals, therefore, providing them with a calibration or 0.11‰ $\delta^{18}O$ for each 10 meters of change in sea level. They then used the $\delta^{18}O$ to sea level calibration to constrain relative sea level from $\delta^{18}O$ from 80,000 to 220,000 years.

Calibrating isotopes to glacioeustasy from pre-quaternary records

The following section is modified from Pekar et al. (2006), Pekar and DeConto (2006) and Pekar and Christie-Blick (in press). The first calibration of $\delta^{18}O$ to quantitative eustatic estimates for pre-Quaternary records was accomplished by Pekar et al. (2002) using backstripped Oligocene stratigraphy from New Jersey. Ice-volume changes and their associated changes in sea level were determined by calibrating amplitudes of apparent sea level (ASL, defined as eustasy plus water loading effects) to $\delta^{18}O$ amplitudes for isotopic-events identified by Miller et al. (1991) and Pekar and Miller (1996) in deep-sea records (Pekar et al., 2002, 2006; Pekar and DeConto, 2006). Each calibration is based on linear regression of records from individual sites (Pekar et al., 2002; 2006) (Figure 18). They range from 0.12-13‰/10 m ASL for Weddell Sea ODP Sites 689 and 690 to 0.20‰/10 m for southern Atlantic Ocean Site 522, 0.23‰/10 m for equatorial Pacific Ocean Site 1218, 0.32‰/10 m for southern Atlantic Ocean Site 1090, and 0.35‰/10 m for Equatorial Atlantic Ocean Site 929.

Differences among the calibrations are attributable to variability in deep-sea temperatures among the sites between glacial maxima and minima at the million-year time scale. Correlation between deep-sea $\delta^{18}O$ and ASL amplitudes is good to excellent for each site, with a correlation coefficient (r^2) for regressions ranging from 0.73 to 0.99 (Pekar et al., 2002, 2006) (Figure 18). This suggests that although deep-sea $\delta^{18}O$ values are assumed to contain a significant bottom-water temperature signal, any temperature lowering scales more or less linearly with respect to increased ice volume (Pekar et al., 2002). The calibrations for Sites 929 and 1090 use a single $\delta^{18}O$ event (Mi1, 23.0 Ma, 56±25 m ASL), which results in an isotopic range of ~0.2 to 0.5‰ (0.35±0.15‰ mean value) and 0.18 to 0.46‰ (0.32±0.14‰ mean value) per 10 m ASL, respectively.

Oligocene $\delta^{18}O$ values of 3‰ or greater in deep-sea records are consistent with an EAIS of modern size and with bottom water temperatures ≤ 2.0˚ C. This is based on the average modern *Cibicidoides* spp. value of 2.7‰ in ~2.0˚ C waters (Shackleton and Kennett, 1975) or 3.34‰ adjusted for equilibrium with calcite. The Greenland Ice Sheet probably was not present during the Oligocene, based upon vegetation evidence for insufficiently cold conditions in the

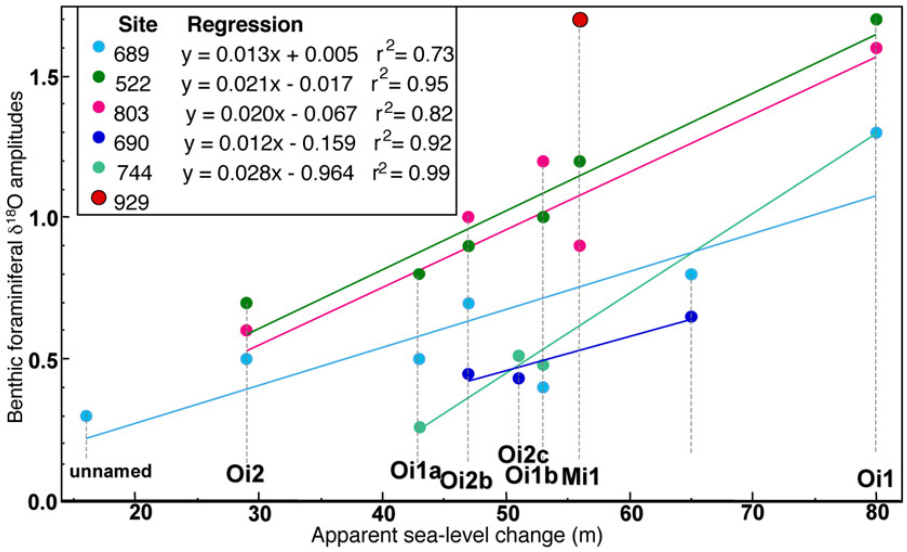

Figure 18. Modified from Pekar et al. (2006). Oxygen isotope amplitudes from Oi-events identified in ODP Sites 690, 689, 744, 929, 1090, and 1218 (Thomas et al., 1995; Zachos et al., 2001; Lear et al., 2004) are compared to detrended ASL amplitudes (Pekar et al., 2002). Oxygen isotope amplitudes are the difference between the maximum value of $\delta^{18}O$ event and preceding minimum (or average minimum) $\delta^{18}O$ value. ASL amplitudes (Pekar et al., 2002) are the difference between sea-level minimum and the preceding sea-level maximum. Oxygen isotope events are shown (Miller et al., 1991; Pekar and Miller, 1996).

northern hemisphere (e.g., Wolfe, 1978), and this would have reduced the average deep-sea $\delta^{18}O$ value by 0.07‰. While the existence in the Oligocene of a substantial West Antarctic Ice sheet is still controversial (Ivany et al., 2006; Rocchi et al., 2006, Sorlien et al., in press), the average deep-sea $\delta^{18}O$ value would be approximately the same in either case (3.02‰ with an ice sheet, and 2.96‰ without; Pekar et al., 2006). Ice in a polythermal EAIS during the Oligocene most likely had significantly higher $\delta^{18}O$ values (e.g., ~ -35‰) than is the case today (i.e., -45‰ to -55‰; DeConto and Pollard, 2003). The existence of higher values is supported by floral evidence for appreciably warmer conditions in the Ross Sea region during the Oligocene than is the case today (> 9°C warmer; Prebble et al., 2006). This would have reduced the mean isotopic value of the oceans by an additional 0.25‰. Taken together, these considerations suggest that an isotopic value of ~3‰ in calcite is consistent with a fully glaciated East Antarctic continent during the Oligocene.

Uncertainties in estimating ice volume from calibrated isotopic records relate to temperature variability that exceeds the calibration for a given site based on the long-term changes in deep-sea circulation patterns as well as in the salinity variations among the sites. During the late Oligocene, for example, a warmer deep-sea water mass is thought to have expanded and replaced a colder water mass at a number of sites in both the Atlantic and Pacific basins (Pekar et al., 2006). While the potential exists for salinity to affect ice-volume estimates from calibrated records, the range in salinity between water masses in the deep sea today (e.g., North Atlantic Deep Water [34.95‰] and Antarctic Bottom Water, AABW [34.65‰]) is about 0.3‰, resulting in an isotopic uncertainty of only ±0.1‰. The lower $\delta^{18}O$ value associated with lower salinity cold deep water such as proto-AABW is equivalent to an underestimate of ice volume. In our analysis, offsets between calibrations among the different sites are ascribed to temperature variability between ocean basins. For example, $\delta^{18}O$ values for Mi1 that are ~0.4‰ lighter at Sites 929 and 1218 than at Site 1090 are attributed to colder bottom water at the latter, and are adjusted accordingly.

Calibrated isotopic records

Calibrated isotopic records provide a new means for estimating Paleogene ice volume, with a high degree of confidence based on the good to excellent correlation in calibrations. This approach circumvents a shortcoming of alternative methods, such as the use of covariance between $\delta^{18}O$ records from tropical planktonic and deep-sea benthic foraminifers assuming little to no temperature signal in planktonic $\delta^{18}O$ values. Indeed, Pleistocene data for tropical surface-dwelling planktonic foraminifers indicate substantial temperature changes (2˚ C), equivalent to ~50 m ASL change between glacial and interglacial periods (Guilderson et al., 1994). Therefore, ice volume estimates using this approach can only provide a maximum value (see Lear and Pekar chapter, this book).

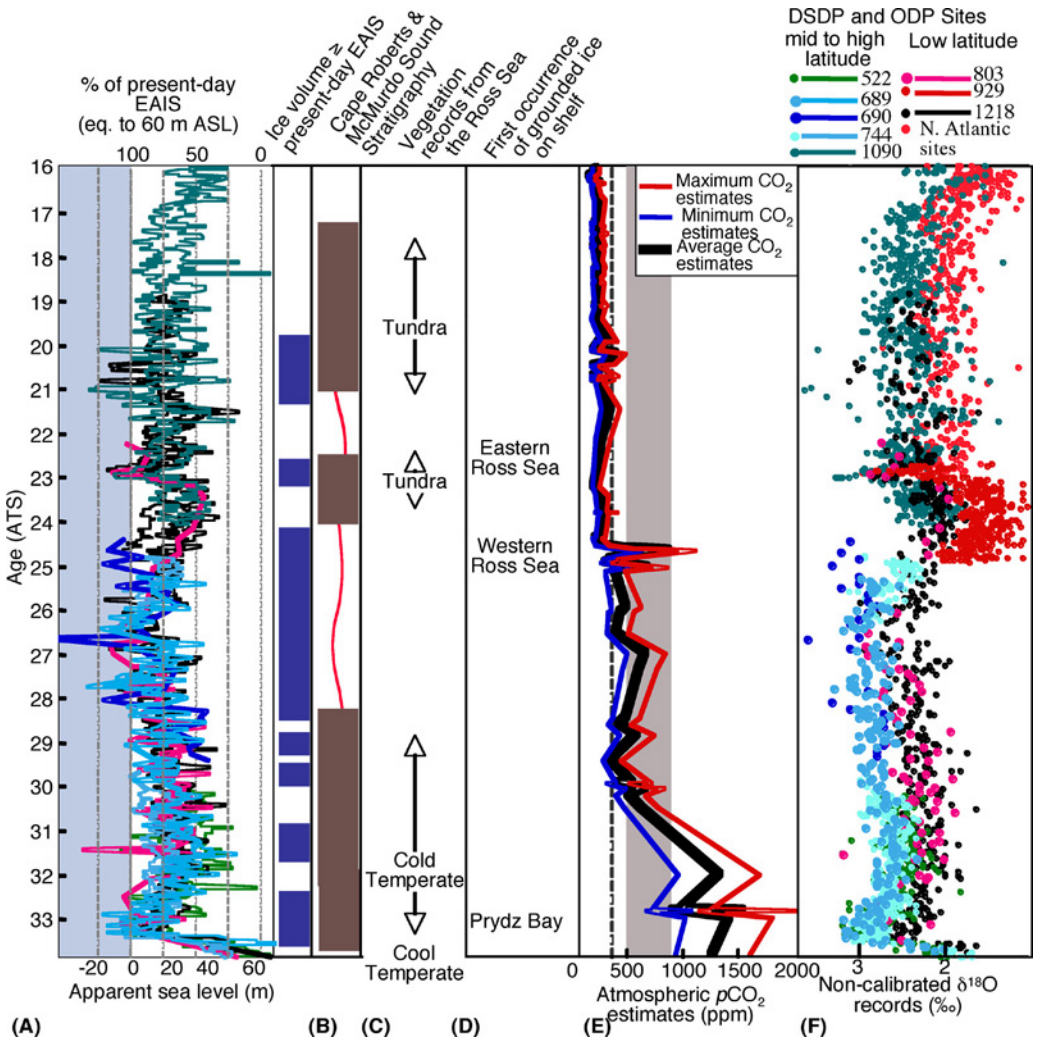

Figure 19. Modified from Pekar and Christie-Blick, in press. (A) Apparent sea-level (ASL) estimates are derived by applying $\delta^{18}O$ to ASL calibrations to $\delta^{18}O$ records (Pekar et al., 2002; Pekar et al., 2006) from Deep Sea Drilling Program and Ocean Drilling Program Sites 522, 689, 690, 744, 803, 929, 1090, and 1218. The upper x-axis is the percent of the present-day EAIS (equivalent to ~60 m ASL). The lower x-axis is ASL change, with zero representing sea level resulting from ice volume equivalent to the present-day EAIS, with increasing values representing sea-level rise and negative numbers representing ice volume greater than the present-day EAIS volume. Thick blue lines represent times when ice volume was ≥ than present-day EAIS based on calibrated isotopic records. (B) The composite stratigraphy of cores from the Cape Roberts Project that were drilled in the western Ross Sea. Thick brown lines represent times when sediment was preserved and red wavy lines represent times of hiatuses identified in cores (based on the chronology of Florindo et al., 2005). Note the excellent agreement when ice volume was ≥ than present-day EAIS and the timings of the hiatuses. (C) Biological data from Antarctica (Askin, 2001). (D) First occurrence of grounded ice based on core and seismic data around Antarctica (Cooper et al., 1991; Hambrey et al., 1991; Bartek et al., 1997; Chow and Bart, 2003). (E) pCO_2 estimates from Pagani et al. (2005) show decreasing values during the Oligocene reaching pre-industrial levels by the latest Oligocene and continuing into the early Miocene. (F) Deep-sea $\delta^{18}O$ composite modified from Zachos et al. (2001), which includes Sites 803 (Barrera et al., 1993), 1090 (Billups et al., 2002), and 1218 (Lear et al., 2004). The abrupt $\delta^{18}O$ decrease at circa 24.5 Ma is due to a change in the source of data from high latitude to low latitude sites, with Southern Ocean sites below and mainly western equatorial Atlantic Site 929 above (Pekar et al. 2002; Pekar et al., 2006).

Calibrated isotopic records indicate that ice volume increased from near zero during the late Eocene to 25% larger than the present-day EAIS (equivalent to an ASL lowering of 75 m) by the earliest Oligocene (33.5 Ma; Figure 19). Oligocene ice volume was greatest at ~29 and 25 Ma, being some 30% larger than the present-day EAIS (equivalent to

80 m of ASL lowering). The EAIS was generally smaller between 33 and 29 Ma (with the exception of isotope event Oi1b [31.7-31.4 Ma]) and between 26 and 23.2 Ma, with ice volume during glacial maxima close to 80% of the present-day EAIS. Our calibrated records also show that ice volume rarely decreased below 50% of the present-day EAIS during Oligocene glacial minima, except between 32.3 and 30.1 Ma and between 24.0 and 23.2 Ma, with ice volume as low as 30-40% of the modern EAIS.

Ice volume during most of the early Miocene (23-16 Ma) was comparable to that of the Oligocene, ranging from 50 to 130% of the present-day EAIS (Pekar and DeConto, 2006), with the possibility of brief episodes (< 100 ky duration) of lower ice volume. These estimates, which are consistent with paired Mg/Ca ratio and isotopic evidence for ice volumes 30 to 50% larger than the present-day EAIS (equivalent to 70-90 m of ASL change; Lear et al., 2000, 2004), suggest that at glacial maxima the ice sheet would have extended seaward of the present-day coastline and across at least part of the continental shelf. At glacial minima, the ice sheet would have retreated as much as several hundred kilometers inland of the modern coastline.

References

Askin, C.B., 2001, Glacial influence from clast features in Oligocene and Miocene strata cored in CRP-2A and CRP-3, Victoria Land Basin, Antarctica: Terra Antartica, 7:493-501.

Bandy, O. L., 1953, Ecology and paleoecology of some California foraminifera; Part I, The frequency distribution of Recent foraminifera off California: Journal of Paleontology, 22:161-182.

Bandy, O.L., 1961, Distribution of foraminifera, radiolaria, and diatoms in sediments of the Gulf of California: Micropaleontology, 7:1-26.

Bandy, O.L., 1964, General correlation of foraminiferal structure with environment, *in* Imbrie, J., and Newell, N., eds Approaches to Paleoecology: New York, Wiley and Sons, p. 75-90.

Bandy, O.L., and Arnal, R., 1957, Distribution of recent foraminifera off the west coast of Central America: American Association of Petroleum Geologists, Bulletin, v. 41, p. 2037-2053.

Bandy, O.L., and Arnal, R., 1960, Concepts in foraminiferal paleoecology: American Association of Petroleum Geologists, Bulletin, 44:921-1932.

Barrera, E., Baldauf, J., Lohmann, K.C., 1993, Strontium isotope and benthic foraminifer stable isotopic results from Oligocene sediments at Site 803, In: Berger, W.H., Kroenke, L.W., Mayer, L.A., (Eds.), Proceedings of the Ocean Drilling Program, Scientific Results 130, Ocean Drilling Program, College Station, pp. 269-279.

Barrett, P.J. (Ed.), 1989, Antarctic Cenozoic history from CIROS-1 Drillhole, McMurdo Sound. Bulletin vol. 245. Department of Scientific and Industrial Research, Scientific Information Publishing Centre, Wellington, New Zealand, pp. 1-254.

Bartek, L.R., Andersen, J.L.R., Oneacre, T.A., 1997, Substrate control on distribution of subglacial and glaciomarine seismic facies based on stochastic models of glacial seismic facies deposition on the Ross Sea continental margin, Antarctica: Marine Geology, 143:223-262.

Billups, K., Channell, J.E.T., Zachos, J., 2002, Late Oligocene to early Miocene geochronology and paleoceanography from the subantarctic South Atlantic. Paleoceanography 17, 10.1029/2000PA000568.

Bond, G. C., 1979, Evidence for late Tertiary uplift of Africa relative North America, South America, Australia, and Europe: Journal of Geology, 86:47-65.

Bond, G. C., and Kominz, M. A., 1984, Construction of tectonic subsidence curves for the early Paleozoic miogeocline, southern Canadian Rocky Mountains: Implications for subsidence mechanisms, age of breakup, and crustal thinning: Geological Society of America Bulletin, 95:155-173.

Bowman, M.J., 1977, Hydrographic Properties: New York Sea Grant Institute, Albany, New York, 78 p.

Browning, J.V., Miller, K.G., and Bybell, L.M., 1997, Upper Eocene sequence stratigraphy and the Absecon Inlet Formation, New Jersey Coastal Plain, *in* Miller, K.G., and Snyder, S.W., eds., Proceedings of the Ocean Drilling Program, Scientific Results, 150X:243-266.

Chow, J.M., Bart, P.J., 2003, West Antarctic Ice Sheet grounding events on the Ross sea outer continental shelf during the middle Miocene: Palaeogeography, Palaeoclimatology, Palaeoecololgy, 198:169-186.

Christie-Blick, N., 1991, Onlap, offlap, and the origin of unconformity-bounded depositional sequences: Marine Geology, 97:35-56.

Christie-Blick, N., and Driscoll, N. W., 1995, Sequence stratigraphy: Annual Review of Earth and Planetary Science, v. 23, p. 451-478.

Greenlee, S. M., and Moore, T. C., 1988, Recognition and interpretation of depositional sequences and calculation of sea-level changes from stratigraphic data- offshore New Jersey and Alabama Tertiary: *in* Wilgus, C. K., Posamentier, H., Ross, C.A., and Kendall, C. G. St. C., eds., Sea-level changes: An integrated approach: Society of Economic Paleontologists and Mineralogist, Special Publication No. 42, p. 329-353.

Cooper, A.K., Barrett, P.J., Hinz, K., Traube, V., Leitchenkov, G., Stagg, H.M.J., 1991, Cenozoic prograding sequences of the Antarctic continental margin: A record of glacio-eustatic and tectonic events: Marine Geology 102:175-213.

DeConto, R.M., Pollard, D., 2003, Rapid Cenozoic glaciation of Antarctica induced by declining atmospheric CO2: Nature, 421:245-249.

Florindo, F., Wilson, G.S., Roberts, A.P., Sagnotti, L., Verosub, K.L., 2005, Magnetostratigraphic chronology of a late Eocene to early Miocene glacimarine succession from the Victoria basin, Ross Sea, Antarctica: Global and Planetary Change, 45:207-236.

Guilderson, T. P., Fairbanks, R. G., Rubenstone, J. L., 1994, Tropical temperature variations since 20,000 years ago: Modulating interhemispheric climate change: Science, 263:663-665.

Hambrey, M.J., Ehrmann, W.U., Larsen, B., 1991, Cenozoic glacial record of the Prydz Bay continental shelf, East Antarctica. In: Barron, J., et al. (write out all editors) (Eds.), Proceedings of the Ocean Drilling Program, Scientific Results 119, Ocean Drilling Program, College Station, Texas, pp. 77-132.

Haq, B.U., Hardenbol, J., Vail, P.R., 1987, Chronology of fluctuating sea levels since the Triassic: Science, 235:1156-1167.

Harrison, C.G.A., III, 1990, Long term eustasy and epeirogeny in continents, *in*: Revelle, R., ed., Sea-Level Change, Washington, DC, National Academy of Sciences, p. 141-158.

Hayward, B.W., Grenfell, H.R., Reid, C.M., and Hayward, K.A. 1999, Recent New Zealand shallow-water benthic foraminifera: Taxonomy, ecologic distribution, biogeography, and use in paleoenvironmental assessment: Institute of Geological and Nuclear Sciences, New Zealand, Monograph 21, 258 p.

Ivany, L.C., Van Simaeys, S., Domack, E.W., and Samson, S.D., 2006, Evidence for an earliest Oligocene ice sheet on the Antarctic Peninsula: Geology, 34:377-380.

Kominz, M. A., 1984, Oceanic ridge volumes and sea level change - An error analysis, *in* Schlee, J., ed., Interregional unconformities and hydrocarbon accumulation: Tulsa, Oklahoma, American Association of Petroleum Geologists, Memoir No. 36, p. 109-127.

Kominz, M. A., Miller, K. G., and Browning, J. V., 1998, Long-term and short term global Cenozoic sea-level estimates: Geology, 26:311-314.

Kominz, M.A., Pekar, S.F., 2001, Oligocene eustasy from two-dimensional sequence stratigraphic backstripping: Geological Society of America Bulletin, 113:291-304.

Kominz, M.A., Pekar, S.F., 2002, Testing the tenets of sequence stratigraphy: In 22nd Annual GCSSEPM Foundation Bob F. Perkins Research Conference, Sequence Stratigraphic Models for Exploration and Production: Evolving Methodology, Emerging Models and Application Case Histories, p. 349-365.

Lear, C.H., Elderfield, H., Wilson, P.A., 2000, Cenozoic deep-sea temperature and global ice volumes from Mg/Ca in benthic foraminiferal calcite: Science, 287:269-272.

Lear, C.H., Rosenthal, Y., Coxall, H.K., Wilson, P.A., 2004, Late Eocene to early Miocene ice sheet dynamics and the global carbon cycle: Paleoceanography, 19, PA4015, doi:10.1029/2004PA001039.

Lipps, J.H., Berger, W.H., Buzas, M.A., Douglas, R.G., and Ross, C.A., 1979, Foraminiferal Ecology and Paleoecology: Society of Economic Paleontologists and Mineralogists, Short Course 6, 198 p.

McKenize, D., 1978, Some remarks on the development of sedimentary basins: Earth and Planetary Science Letters, 40:25-32.

Miller, K. G., and Fairbanks, R. G., 1985, Cainozoic ∂^{18}O record of climate and sea level: South African Journal of Sciences, 81:248-249.

Miller, K. G., Fairbanks, R. G., and Mountain, G. S., 1987, Tertiary oxygen isotope synthesis, sea-level history, and continental margin erosion: Paleoceanography, v. 2, p. 1-19.

Miller, K.G., Wright, J.D., Fairbanks, R.G., 1991, Unlocking the ice house: Oligocene-Miocene oxygen isotopes, eustasy, and margin erosion: Journal of Geophysical Research, 96:6,829-6,848.

Miller, K. G., Mountain, G. S., Blum, P, Gartner, S, Alm, P.G., Aubry, M.P., Burckle, L. H., Guerin, G, Katz, M. E., Christensen, B. A., Compton, J, Damuth, J. E., Deconinck, J. F., de Verteuil, L, Fulthorpe, C. S., Hesselbo, S. P., Hoppie, B. W., Kotake, N., Lorenzo, J. M., McCracken, S, McHugh, C. M., Quayle, W. C., Saito,Yoshiki, S., S. W., ten Kate, W. G., Urbat, M., Van Fossen, M. C., Vecsei, A., Sugarman, P. J., Mullikin, L, Pekar, S., Browning, J. V., Liu, C., Feigenson, M. D., Goss, M., Gwynn, D., Queen, D. G., Powars, D. S., Heibel, T. D., Bukry, D., 1996, Drilling and dating New Jersey Oligocene-Miocene sequences; ice volume, global sea level, and Exxon records: Science, 271:1,092-1,095.

Miller, K. G., Browning, J. V., Pekar, S. F., and Sugarman, P. J., 1997, Cenozoic evolution of the New Jersey Coastal Plain: changes in sea level, tectonics, and sediment supply, *in* Miller, K. G., and Snyder, S. W., eds., Scientific Results of the Ocean Drilling Program., Volume 150X: Washington, D.C., U.S. Government Printing Office, p 361-373.

Miller, K.G., Rufolo, S., Sugarman, P.J., Pekar, S.F., Browning, J.V., and Gwynn, D.W., 1997, Early to middle Miocene sequences, systems tracts, and benthic foraminiferal biofacies: Proceedings of the Ocean Drilling Program, Scientific Results, 150X:169-186.

Miller, K. G., Mountain, G.S., Browning, J. V., Kominz, M. A., Sugarman, P. J., Chrisite-Blick, N., Katz, M. E., and Wright, J. D., 1998b, Cenozoic global sea-level, sequences, and the New Jersey Transect: results from coastal plain and slope drilling: Reviews of Geophysics. 36: 569-601.

Miller, K. G. and Sugarman, P. J., et al., 1998a, Bass River Site Report: Initial Reports, New Jersey Coastal Plain, Ocean Drilling Program, Leg 174AX: College Station, Texas, Ocean Drilling Program, 43p.

Miller, K.G., Kominz, M.A., Browning, J.V., Wright, J.D., Mountain, G.S., Katz, M.E., Sugarman, P.J., Cramer, B.S., Christie-Blick, N., Pekar, S.F., 2005, The Phanerozoic record of global sea-level change: Science, 312:1293-1297.

Murray, J.W., 1973, Distribution and ecology of living benthic foraminferids: New York, Crane, Russak and Co., 274 p.

Nyong, E. O., and Olsson, R. K., 1984, A paleo-slope model of Campanian to Lower Maestrictian foraminifera in the North American basin and adjacent continental margin: Marine Micropaleontology, 8:437-477.

Olsson, R. K., 1991, Cretaceous to Eocene sea-level fluctuations on the New Jersey margin: Sedimentary Geology, 70:195-208.

Pagani, M., Zachos, J.C., Freeman, K.H., Tipple, B., Bohaty, S., 2005, Marked decline in atmospheric carbon dioxide concentrations during the Paleogene: Science, 309:600-603.

Pekar, S. F., and Miller, K. G., 1996, New Jersey Oligocene "Icehouse" sequences (ODP Leg 150X) correlated with global δ^{18}O and Exxon eustatic records: Geology, 24:567-570.

Pekar, S.F., 1999, A New Method for Extracting Water Depth, Relative Sea-Level, and Eustatic Records From Onshore New Jersey Oligocene Sequence Stratigraphy [unpublished Ph.D. thesis]: Rutgers University, Piscataway, 182 p. Pekar, S., Miller, K.G., 1996, New Jersey Oligocene "Icehouse" sequences (ODP Leg 150X) correlated with global δ^{18}O and Exxon eustatic records: Geology, 24:567-570.

Pekar, S.F., Miller, K.G., and Browning, J.V., 1997, New Jersey coastal plain Oligocene sequences, *in* Miller, K.G., and Snyder, S.W., eds., Proceedings of the Ocean Drilling Program, Scientific Results, 150X:187-206.

Pekar, S.F., Miller, K.G., and Kominz, M.A., 2000, Reconstructing the stratal geometry of New Jersey Oligocene sequences: resolving a patchwork distribution into a clear pattern of progradation: Sedimentary Geology, 134:93-109.

Pekar, S.F., Kominz, M.A., 2001, Two-dimensional paleoslope modeling: a new method for estimating water depths for benthic foraminiferal biofacies and paleo shelf margins: Journal of Sedimentary Research, 71:608-620.

Pekar, S.F., Christie-Blick, N., Kominz, M.A., Miller, K.G., 2002, Calibrating eustasy to oxygen isotopes for the early icehouse world of the Oligocene: Geology, 30:903-906.

Pekar, S. F., DeConto, R.M., 2006, High-resolution ice-volume estimates for the early Miocene: Evidence for a dynamic ice sheet in Antarctica: Palaeogeography, Palaeoclimatology, Palaeoecology, 231:101-109.

Pekar, S.F., Harwood, D.M., DeConto, R.M., 2006, Resolving a late Oligocene conundrum: deep-sea warming versus Antarctic glaciation: Palaeogeography, Palaeoclimatology, Palaeoecology, 231:29-40.

Pekar, S.F., Christie-Blick, N., 2007, Resolving apparent conflicts between oceanographic and Antarctic climate records and evidence for a decrease in pCO_2 during the Oligocene through early Miocene (34-16 Ma): Palaeogeography, Palaeoclimatology, Palaeoecology, in press.

Prebble, J.G., Raine, J.I., Barrett, P.J., Hannah, M.J., 2006, Vegetation and climate from two Oligocene glacioeustatic sedimentary cycles (31 and 24 Ma) cored by the Cape Roberts Project, Victoria Land Basin, Antarctica: Palaeogeography, Palaeoclimatology, Palaeoecology, 231:41-57.

Reynolds, D. J., Steckler, M. S., and Coakley, B. J., 1991, The role of the sediment load in sequence stratigraphy: the influence of flexural isostasy and compaction: Journal of Geophysical Research, 96:6931-6949.

Rhodehamel, E. C., 1977, Sandstone porosities, *in* Scholle, P. A., ed., Geological studies on the COST No. B-2 well, U.S. mid-Atlantic outer continental shelf area: U.S. Geological Survey Circular 750, p. 23-31.

Rocchi, S., LeMasurier, W.E., Di Vincenzo, G., 2006, Oligocene to Holocene erosion and glacial history in Marie Byrd Land, West Antarctic, inferred from exhumation of the Dorrel Rock intrusive complex and from volcano morphologies: Geological Society of America Bulletin, 118:991-1005.

Sen Gupta, B. K., 1971, The benthonic foraminifera of the tail of the Grand Banks: Micropaleontology, v. 17, p. 69-98.

Schalanger, S. O., Jenkyns, H. C. and Premoli-Silva, I., 1981, Volcanism and vertical tectonics in the Pacific Basin related to global Cretaceous transgressions: Earth and Planetary Science Letters, v. 52, p. 435-449.

Sahagian, D. L., 1988, Ocean temperature-induced change in lithospheric thermal structure: A mechanism for long-term eustatic sea level change: Journal of Geology, 96:254-261.

Sahagian, D. L., and Jones, M., 1993, Quantified Mid-Jurassic through Paleogene eustatic variations based on Russian platform stratigraphy: Stage-level resolution: Geological Society of America Bulletin, 105:1109-1118.

Shackleton, N.J., Kennett, J.P., 1975, Late Cenozoic oxygen and carbon isotopic changes at DSDP Site 284: Implications for glacial history of the Northern Hemisphere and Antarctic. In: Kennett, J.P., Houtz, R.E., et al. (Eds.), Initial Reports of the Deep Sea Drilling Project 29, Washington (US Government Printing Office), pp. 801-808.

Smith, M. A., Amato, R. V., Furbush, M. A., Pert, D. M., Nelson, M. E., Hendrix, J. S., Tamm, L. C., Wood, G., Jr., and Shaw, D. R., 1976, Geological and operational summary, COST No. B-2 well, Baltimore Canyon Trough area, Mid-Atlantic OCS: U.S. Geological Survey Open-File Report 76-774, 79p.

Sorlien, C. C., Luyendyk, B. P., Wilson, D., Decesari, R., Bartek, L., Diebold, J., 2007, Oligocene developments of the West Antarctic Ice Sheet recorded in eastern Ross sea strata: Geology, 35: 467–470.

Steckler, M. S., Mountain, G. S., Miller, K. G., and Christie-Blick, N. 1999, Reconstruction of Tertiary progradation and clinoform development on the New Jersey passive margin by 2-D backstripping: Marine Geology, 154:399-420.

Steckler, M. S., Watts, A. B., and Thorne, J. A., 1988, Subsidence and basin modeling at the U.S. Atlantic passive margin, *in* Sheridan, R. E., and Grow, J. A., eds., The Atlantic Continental Margin: U.S.: Boulder, Colorado, Geological Society of America, The Geology of North America, v. I-2, p. 399-416.

Stehli, F., and Creath, W., 1964, Foraminiferal ratios and regional environments: American Association of Petroleum Geologists, Bulletin, 48:1810-1827.

Thomas, E., Zahn, R., Diester-Hauss, L., 1995, The Eocene-Oligocene transition at high latitudes: benthic foraminifera, sediments and stable isotopes. EOS Transactions 76 Supplement, pp. S187.

Vail, P. R., and Mitchum, R. M., Jr., 1977, Seismic stratigraphy and global changes of sea-level, Part 1: Overview, *in* Payton, C. E., ed., Seismic stratigraphy - Applications to Hydrocarbon Exploration: Tulsa, Oklahoma, American Association of Petroleum Geologists, Memoir No. 26, p. 51-52.

Van Hinte, J.E., 1978, Geohistory analysis: Application of micropaleontology in exploration geology: AAPG Bulletin, 62:201-222.

Walton, W.R., 1964, Recent foraminiferal ecology and paleoecology *in* Imbrie, J. and Newell, N., eds., Approaches to Paleoecology: New York, John Wiley, p. 151-237.

Watts, A. B., and Steckler, M. S., 1979, Subsidence and eustasy at the continental margin of eastern North America, *in* Talwani, M., Hay, W., and Ryan, W. B. F., eds., Deep drilling results in the Atlantic Ocean; continental margins and paleoenvironment: Washington, D.C., American Geophysical Union, Maurice Ewing Series No. 3, p. 218-234.

Zachos, J. C., Rea, D. K., Seto, K., Niitsuma, N., and Nomura, R., 1992, Paleogene and early Neogene deep water history of the Indian Ocean: inferences from stable isotopic records, *in* Duncan, R. A., Rea, D. K., Kidd, R. B., von Rad, U., and Weissel, J. K., eds., The Indian Ocean: A Synthesis of Results from the Ocean Drilling Program: American Geophysical Union, Geophysical Monograph, 70:351-386.

Zachos, J.C., Pagani, M., Sloan, L., Thomas, E., Billups, K., 2001, Trends, rhythms and aberrations in global climate 65 Ma to present: Science, 292: 686-693.